Journal of Plant Growth Regulation (2026) 45:3741–3756
https://doi.org/10.1007/s00344-026-12107-0

Early-onset Dynamics of Arbuscular Mycorrhizal Symbiosis Reprogram Metabolic and Physiological Responses in Tomato Roots

Ilaria Ragnoli[1] · Leilei Zhang[1] · Florencia Asinari[2,3] · Tito Caffi[2,4] · Luigi Lucini[1]

Received: 4 August 2025 / Accepted: 9 February 2026 / Published online: 19 February 2026

Abstract

Arbuscular mycorrhizal fungi (AMF) are widely utilized in agriculture to enhance plant fitness. However, the processes underlying symbiosis establishment remain poorly understood. This study investigates the dynamics of mycorrhization in tomato plants (*Solanum lycopersicum* L.) over one month in environmentally controlled condition, integrating metabolomics analysis of roots and root exudates with phenotypic traits, including morphological (RGB imaging) and physiological (fluorescent imaging) analyses to study the onset of symbiotic relationships when AMF were applied at either seeding or post-germination. The results revealed that AMF reduced root system growth at one-month post-germination but enhanced photosynthetic efficiency (Fv/Fm), suggesting a "metabolic cost" induced by the fungal association. Notably, the shoot/root ratio significantly increased by 102% in seed-treated and 45% in post-germination inoculated plants. Interestingly, AMF decreased tomato performance during the early stages of development compared to their untreated counterparts. Shoot biomass decreased by 30% and 25% under seed priming and fungal inoculation, respectively. The development of the root system was also adversely affected, with an average reduction in biomass of 35% and in length of 31%. Metabolomics results indicate that AMF slows initial plant growth to facilitate the establishment of symbiosis, pushing resources towards secondary metabolism and exudation of recruiting compounds. Application methods influenced early-stage physiological responses, with post-germination inoculated plants exhibiting higher "metabolic cost" than seed-primed counterparts. Mycorrhization in tomato was fully established approximately 27 days after AMF treatment.

Highlights

- Early AMF colonization imposes a metabolic cost, delaying physiological recovery.
- Seed priming facilitates gradual symbiotic onset, reducing metabolic disruption.
- AMF influences plant metabolism, modulating biosynthetic pathways and exudation profiles.
- Symbiosis fully establishes after 27 days, influencing microbiome composition.
- Resource allocation shifts toward secondary metabolism and recruitment compounds.

Keywords Photosynthetic efficiency · Root exudation · Secondary metabolism · Plant holobiont · Arbuscular fungi.

Communicated by Axel Mithöfer

✉ Leilei Zhang
leilei.zhang@unicatt.it

[1] Department for Sustainable Food Process, Università Cattolica del Sacro Cuore, Piacenza, Italy

[2] Department of Sustainable Crop Production, Università Cattolica del Sacro Cuore, Piacenza, Italy

[3] Instituto de Patología Vegetal, Instituto Nacional de Tecnología Agropecuaria, Consejo Nacional de Investigaciones Científicas y Técnicas, Unidad de Fitopatología y Modelización Agrícola, Córdoba, Argentina

[4] Research Center on Plant Health Modelling, Department of Sustainable Crop Production, Università Cattolica del Sacro Cuore, Piacenza, Italy

Introduction

The world population has faced an unprecedented climate crisis in recent years, which has also heavily hit the agricultural sector (Malhi et al. 2021). These conditions have affected food crops, limiting their production and product quality. This contrasts with the current population growth, a steadily growing phenomenon estimated to reach nearly 10 billion people by 2050 (Malhi et al. 2021). Therefore, food security is a problem of great importance at a global level, and solutions to ensure it must be taken as soon as possible. An increasingly widespread approach to stimulating plant productivity is the use of biostimulants, which are microbial and non-microbial substances that have been shown to increase crop resistance to various climate change-driven stresses (Calvo et al. 2014). Since most products have a natural origin (Johnson et al. 2024), their processing and use have a minimal environmental impact, while improving nutrient use efficiency and tolerance to abiotic stress in plants. In this context, the employment of arbuscular mycorrhizal fungi (AMF) has been shown by several studies to help almost all land plants tolerate and resist adverse biotic and abiotic conditions (Wahab and Wu 2023; Delaeter et al. 2024). The most widely used AMF species belong to the *Glomeromycota* phylum, which is naturally present in soils and can form symbiotic relationships with the roots of many agricultural plants, such as potatoes, maize, and tomato (Arcidiacono et al. 2024). When AMF is administered exogenously to plants, it can be implemented through different methodologies, each influencing the effects of mycorrhizae on plant health and development. This symbiotic relationship significantly impacts overall plant performance, as plants rely on carbon sources for the development and functioning of AMF (Bravo et al. 2017). Initially, this interaction may lead to a deregulation of photosynthesis activity, resulting in an increased photosynthesis rate to counterbalance the metabolic costs associated with the establishment of symbiosis (Delaeter et al. 2024). In return, this association enables plants to access more essential nutrients from the soil, such as phosphorus and nitrates, thus improving overall plant growth (Gianinazzi et al. 2010; Corradi and Bonfante 2012).

The colonisation of plants by AMF requires extensive reprogramming of the root system, during which the fungus establishes specialised intracellular structures known as arbuscules. While this process shares fundamental characteristics with pathogenic fungal invasion, only AMF provide the plant with valuable nutrients in return, fostering a mutually beneficial symbiotic relationship (Corradi and Bonfante 2012). One of the primary implications of AMF colonisation is the modification of root morphology, resulting in the development of a complex and extensive extraradical hyphal network within the soil that facilitates the acquisition of nutrient and water acquisition. These changes includes the increase of branching can provide additional colonisation sites and improve the structural interface between roots and the fungal network, thereby supporting the overall efficiency of the symbiosis (Cargill et al. 2025).

As already seen in previous works, the relationship with mycorrhizal fungi can modify some growth-related parameters in different plant species, such as yield (Arcidiacono et al. 2024) and photosynthetic activity (Kaschuk et al. 2009). Thus, it is essential to assess these parameters over the plant's lifespan to emphasize the positive impact that mycorrhiza can provide. A promising technology for evaluating plants' growing parameters and photosynthetic activity during the growing time and in a non-destructive manner is the employment of a phenotyping system. This system leads to the analyses of the main photosynthetic parameters, such as the yield of photosystem II (ϕPSII) and the non-photochemical quenching (NPQ) values; furthermore, it also evaluates the leaf area of the plant, which is examined in its entirety and different growth phases (Paul et al. 2019). This approach, coupled with metabolomic analysis, allows us to comprehensively observe the overall changes that symbiosis brings to the plant. Despite the many positive aspects of the interaction between AMF and plants, this symbiotic relationship still requires the plant to consume between 4% and 20% of the fixed carbon (Kiers and Van Der Heijden 2006). The benefits of the AMF-plant interaction become apparent when the mycorrhization in the roots is complete; therefore, many studies focus on periods longer than a month to evaluate these effects (Kaya et al. 2003; Wu et al. 2011; Bona et al. 2017).

Despite the well-established benefits of AMF in enhancing plant fitness, little is known about the early interactions between AMF and plant roots, specifically, the transition from inoculation to complete symbiotic association. A detailed investigation of this process is essential to assess the effects of mycorrhization across different stages of plant development.

To address this gap, we examined the onset of AMF colonization in tomato plants (*Solanum lycopersicum*) using a commercial AMF formulation containing *Rhizoglomus irregulare* BEG72 and *Funneliformis mosseae* BEG234 (Aegis Sym Irriga®). The study was guided by the following hypotheses: (1) AMF inoculation initially suppresses root and shoot growth as part of the symbiotic establishment phase. (2) AMF enhances photosynthetic efficiency once colonization is fully established, improving plant physiological performance. (3) The timing and method of AMF application (seed priming vs. post-germination inoculation) influence the rate and success of symbiosis development. To validate these hypotheses, we analyzed tomato plants by

means of a combination of morphological, molecular, and physiological assessments at different growth stages and their metabolic modulation during mycorrhizal symbiosis. This multifaceted approach allowed to evaluate the interactions between tomato roots and AMF, leading to a deeper understanding of the symbiotic relationship and its impact on plant health and development. Specifically, we compared two AMF application strategies: seed priming and post-germination inoculation, in four developmental stages, to determine which method most effectively facilitates the symbiosis process.

Materials and Methods

Experimental Design and Plant Growth

The experiment was carried out on January 2024 at the Department of Sustainable Food Processes at the Università Cattolica del Sacro Cuore in Piacenza, within a growth chamber with controlled temperature (26 °C) and 70% relative humidity during January and February 2024 (10 h light/14 h dark) using LED lamps (Ambra Elettronica srl, Bolzano Vicentino, Vicenza, Italy) emitting 184 µmol m^{-2} s^{-1} of red, 47.5 µmol m^{-2} $s^{-1}$of white, 65 µmol m^{-2} s^{-1} of blue, and 12 µmol m^{-2} $s^{-1}$of far-red lights.

The experiment followed the completely randomised design and involved two complexity factors, including two methods of AMF application and four harvest time points. Tomato seeds (*Solanum lycopersicum* L.) germinated in square pots (6.5 cm width x 9.5 cm height) filled with agronomical soil comprising 93 g/Kg of clay, 187 g/Kg of silt, and 720 g/Kg of sand. The soil was characterized by 3.9 g/Kg of organic carbon, 6.7 g/Kg of organic matter, and 0.084% of total nitrogen content. Six independent replicates were considered for each treatment to reach 72 pots: 24 plants were treated via seed priming (AMF-S), 24 with inoculation (AMF-I) applied 13 days after sowing (DAS), and 24 plants were grown in the same conditions as the control. Mycorrhization was monitored for 35 days in seed-primed plants and 22 days in inoculated plants. The AMF treatment consisted of a commercial product obtained from Athens, Agrotecnologia Naturales SL (Tarragona, Spain). The product is based on the formulation of *Rhizoglomus irregulare* BEG72 and *Funneliformis mosseae* BEG234 (Aegis Sym irriga®), containing 700 spores g^{-1} each species. The formulations were applied according to label recommendations, namely, one application at 0.1 g per plant.

Sample Collection and Growth Measurements

Four different samplings were performed to monitor the onset of mycorrhization over time, specifically 19, 23, 27, and 35 DAS. For each sampling, data on fresh and dry biomass, root exudates, and root tissues for metabolomics were collected. Roots from three independent replicates for each treatment were collected and gathered, immediately frozen in liquid nitrogen, and stored at −20 °C for metabolomics analysis. The remaining three replicates for each treatment were placed in 30 mL of milliQ water for 3 h to collect their exudates; afterwards, the aerial part was separated from the roots and weighed to determine the fresh and dry weights, after drying for 3 days at 80 °C in an oven. Before drying the root system, root morphology and mycorrhizal colonization analyses were performed.

Root Length and Morphology

Roots from three independent replicates for each treatment were analyzed with the TWAIN interface at 600 dpi and with a scanner (Epson Expression 10000xl) coupled with WinRHIZO™ Pro 2019 software (Regent Instruments Inc, Québec City, Canada). Briefly, the acquisition parameters were set based on the tray's dimensions (30 cm in width x 40 cm in length). The image is collected in grey levels. A first scan of the tray was taken as a background control to remove any scratches in the post-processing analysis. The thoroughly cleaned and untangled roots are then placed on the tray with distilled water for the scan. Acquired images are processed by removing borders and dust in the background. Data were elaborated on the cleaned images to collect data on root total length, root average diameter (AvgDiameter), root volume, and root surface area.

Evaluation of Mycorrhizal Root Colonisation

AMF root colonization was estimated at 19, 23, 27, and 35 DAS of plant growth stages. Root samples were carefully washed to remove adhering soil particles, then processed using a clearing and staining protocol adapted from Giachero et al. (2017) to enhance the quantification capacity of hyphae, vesicles, and arbuscules. The bleaching process was performed by immersion in a 10% (w/v) potassium hydroxide (KOH) solution for 20 min in a thermostatic water bath maintained at 80 °C, facilitating the removal of cytoplasmic contents and root pigments. Once the bleaching process was completed, the solution was removed by rinsing with tap water. The roots were rinsed in 0.1 N hydrochloric acid (HCl) solution for 5 min to neutralise KOH and enhance stain penetration. Once the roots were perfectly whitened, Trypan Blue 0.05% was used to stain the root

tissue. The staining process lasted 5 min in the thermostatic water bath maintained at 89 °C. Afterwards, samples were cooled to room temperature and the dye solution was discarded. The excess dye was removed by repeatedly adding and subsequently eliminating lactoglycerol until a transparent solution was obtained, leaving fungal structures clearly visible within the root cortex. The percentage of AMF root colonization was subsequently estimated using the magnified intersections method according to McGONIGLE et al. (1990), which provides a quantitative and reproducible assessment of mycorrhizal colonization. To ensure representative sampling, ten root fragments (1 cm in length) were randomly selected from the stained root material, mounted on microscope slides, and observed under a compound microscope at 40× magnification in ten different fields of view (FOV), totalling one hundred FOV for each sample and 3600 in the entire test. In each FOV, a mark was made when any mycorrhizal structures (including hyphae, arbuscules, and vesicles) were observed at fixed intervals along their length. Total root colonization (%RC) was then calculated as the proportion of FOV at which mycorrhizal structures were recorded relative to the total FOV examined, providing an estimate of overall mycorrhizal colonization intensity within the root system.

RGB Imaging and Chlorophyll Fluorescence Measurement

Photosynthetic performances of plants were detected through the PlantScreenTM System (Photon System Instruments, Drásov, Czech Republic). The analysis was carried out at 19, 23, 27, and 33 DAS to monitor plant growth rates and chlorophyll fluorescence. Briefly, the manual drawing of the plant mask was depicted using an RGB2 top view camera (GigE PSI RGB, 12.3 Megapixels with 1/2.3" CMOS SENSOR). Before acquiring chlorophyll fluorescence images, plants underwent a 10-minute dark adaptation period. Then, MorphoAnalyzer software (version 1.0.9.6) was used to examine the collected images to assess the total biomass area of the plants. Chlorophyll fluorescence was measured using the FluorCam7 application imaging system (Photon Systems Instruments, 2012, Drásov, Czech 123 Republic). Chlorophyll fluorescence images and induction kinetics were measured on pre-darkened leaves (10 min) using the FluorCam Quenching Act2 protocol. The measured chlorophyll fluorescence intensity images were obtained in false colors, where black is the lowest (zero) and red is the highest fluorescence intensity. Fluorescence images were captured by a camera at 16-bit resolution in 1360 × 1024 pixels. Chlorophyll fluorescence images of parameters F0 and F0' (minimum fluorescence in the dark and the light-adapted states), Fm and Fm' (maximum fluorescence in the dark and the light-adapted states) were recorded during induction kinetics.

Untargeted Metabolomics and Root Exudation Profiling

Root tissues and root exudates were profiled using an ultra-high performance liquid chromatography ion mobility quadrupole time-of-flight mass spectrometry (6560 UHPLC/IM-QTOF-MS mass spectrometer – Agilent®, Santa Clara, CA, USA) following extraction in aqueous methanol (Sudiro et al. 2022). For the extraction of root tissues, 500 mg of nitrogen-frozen roots were mechanically homogenized in 5 mL of methanol: water (80:20 *v*/*v*) with a pestle and mortar. Afterwards, the homogenized tissue was then extracted with an ultrasonic bath (Fisher Scientific model FB120, Pittsburgh, PA, United States) for 15 min at an amplitude of 80%. Finally, the extract was centrifuged at 10,000 x *g* for 10 min at 4 °C (Eppendorf 5810R, Hamburg, Germany), and the supernatant was filtered into glass vials using 0.22 µm cellulose filters. Regarding root exudates, the 30 mL water solution collected was centrifuged at 10,000 x *g* for 30 min at 4 °C, then the supernatant was filtered with 0.22 µm cellulose filters, freeze-dried, and finally resuspended in 0.5 mL of 50% methanol in glass vials for further analysis. For each sample, two technical replicates were examined, making a total of six replicates per experimental group. The plant extracts were injected into UHPLC/IM-QTOF-MS, setting an injection volume of 6 µL. The chromatographic separation was conducted using an Agilent InfinityLab Poroshell 120 pentafluorophenyl (PFP) column (2.1 × 100 mm, 1.9 µm). Annotation of metabolomic data recovered from UHPLC/IM-QTOF-MS was carried out using MS-DIAL software (version 4.90) and two different MS/MS libraries, the Fiehn/Vaniya natural product library and BMDMS-NP (Lee et al. 2020). Data filtering and normalization were performed using Mass Profiler Professional B.12.6 software (Agilent Technologies, Santa Clara, CA, USA). The detected compounds were filtered by frequency, normalized at the 75th percentile, and baselined against the median of all samples as described in the **supplementary materials**.

Statistical Analysis

A one-way analysis of variance (ANOVA) was performed with the post hoc Tukey's Honest Significant Difference (HSD) test ($p < 0.05$) was conducted on all morphological and physiological data using IBM SPSS Statistic 25 software. Statistical differences in root colonization rate were determined with two-way analysis of variance (ANOVA) using the statistical software RStudio (Team 2020), an integrated development environment (IDE) for R (Team 2021).

The means were statistically compared using Tukey's LSD (Least Significant Difference) post-hoc test at a 95% confidence level.

The datasets generated by the untargeted metabolomic profiling were elaborated using unsupervised hierarchical cluster analysis (HCA, Euclidean distance), principal component analysis (PCA) and a one-way ANOVA analysis with Benjamini correction (significance level of $p<0.05$) using Mass Profiler Professional 12.6 (Agilent Technologies). Supervised orthogonal projections to discriminant structures analysis (OPLS-DA; SIMCA 16, Umetrics, Malmo, Sweden) and ANOVA Multiblock Orthogonal Partial Least Squares (AMOPLS) analysis (rAMOPLS package in R v. 4.2.1) approaches were also applied. Finally, variables of importance in projection (VIP or VIP^2) were selected as the main biomarkers representing the discrimination ability of the supervised models. Log fold change (Log FC) analysis was performed to identify upward or downward accumulation trends in each discriminant. More details are provided in the **supplementary materials**.

Results

AMF Interaction Distinctively Modulates Tomato Plant Growth

The growth of the plant was monitored for 35 DAS using the phenotyping instrument by assessing the development of the leaf area of the plant (Fig. 1A-D). The imaging data were further confirmed with destructive measurements, including fresh (FW) and dry weight (DW) biomass for both the aerial parts and the roots of the plant (Fig. 1E-H; **Table S1**), recorded at 19, 23, 27, and 35 DAS. Finally, the tomato shoot-to-root ratio was also determined to assess overall plant development at the sampling points (Fig. 1I-L).

At the 19 DAS, tomato plants treated with AMF showed a significant downshift in plant development, as confirmed through leaf area measurement and shoot biomass for both AMF-S and AMF-I (Fig. 1A and E). The control plants showed a shoot biomass of +57% more than AMF-S and +84% more than AMF-I. The same trend was observed for the roots FW and DW, but without statistical differences. At the 23 DAS, the decrease in plant biomass development driven by AMF was not observed, suggesting a plant recovery mechanism after interaction with AMF. The 27 DAS plants doubled their biomass compared to the 23 DAS time point, suggesting the beginning of the growth phase and the consolidation of mycorrhization. In detail, the AMF-S plants exhibited the same leaf area as the control, compared to the AMF-I plants, where the former showed a statistically lower biomass accumulation (Fig. 1G). In the last sampling point, at 35 DAS, a homogeneous development of the aerial part was observed among the treatments. In contrast, a statistically significant slowdown in the development of root FW was reported under AMF treatments (Fig. 1H**)**. Specifically, the mycorrhized root showed a lower biomass than the untreated one, suggesting differential distribution of sources throughout the plant system.

Onset of AMF Mycorrhization Over time

Tomato root colonization (%RC) was estimated at 5, 9, 13, and 21 days after inoculation (I) and 19, 23, 27, and 35 days after seed priming (S). The ANOVA test showed statistical differences for time and time × treatment factors (p-value < 0.05; Fig. 2). On the contrary, there were no statistically significant differences between the two inoculation methods (I and S).

The %RC over time reported significance starting from 27 DAS, reporting the AMF-S application method having the highest colonized roots compared with AMF-I and the control. This different trend was maintained even at 35 DAS. This result suggests that applying the product directly to the seed at sowing favours the mycorrhization process progressively over time (Fig. 2), reaching a total colonisation level of approximately 14% of RC at 27 DAS.

Photosynthetic Performance Is Affected by AMF Treatment

Plant photosynthetic parameters were assessed at 19, 23, 27, and 35 DAS using the phenotyping instrument through chlorophyll fluorescence measurements, considering maximum (Fv/Fm_{max}) and steady-state quantum yield of light-adapted photosystem II (Fv/Fm_{Lss}), steady-state non-photochemical quenching (NPQ_{Lss}), fluorescence decline ratio in steady-state (Rfd_{Lss}), the difference between instantaneous maximum fluorescence during dark relaxation and instantaneous fluorescence during dark relaxation in the light-adapted state (Fq_{Lss}); peak fluorescence during the initial phase of the Kautsky effect (Fp), and steady-state fluorescence in the light (Ft_{Lss}; **Table S2**).

Generally, no statistical significance was reported over time and between treatments for the parameters RfdLss, FqLss, Fp, and FtLss, suggesting an overall health status of tomato plants. In detail, statistical differences among treatments were highlighted for the photosynthetic efficiency (Fv/Fm_{max}) of tomato plants over 35 DAS (Fig. 3A). Nevertheless, this parameter was reported to be generally optimal, with Fv/Fm_{max} values higher than 0.75 in both treated and untreated plants. At 35 DAS, the photosynthetic performance of the control showed a statistically significant reduction, indicating the onset of a general stress condition.

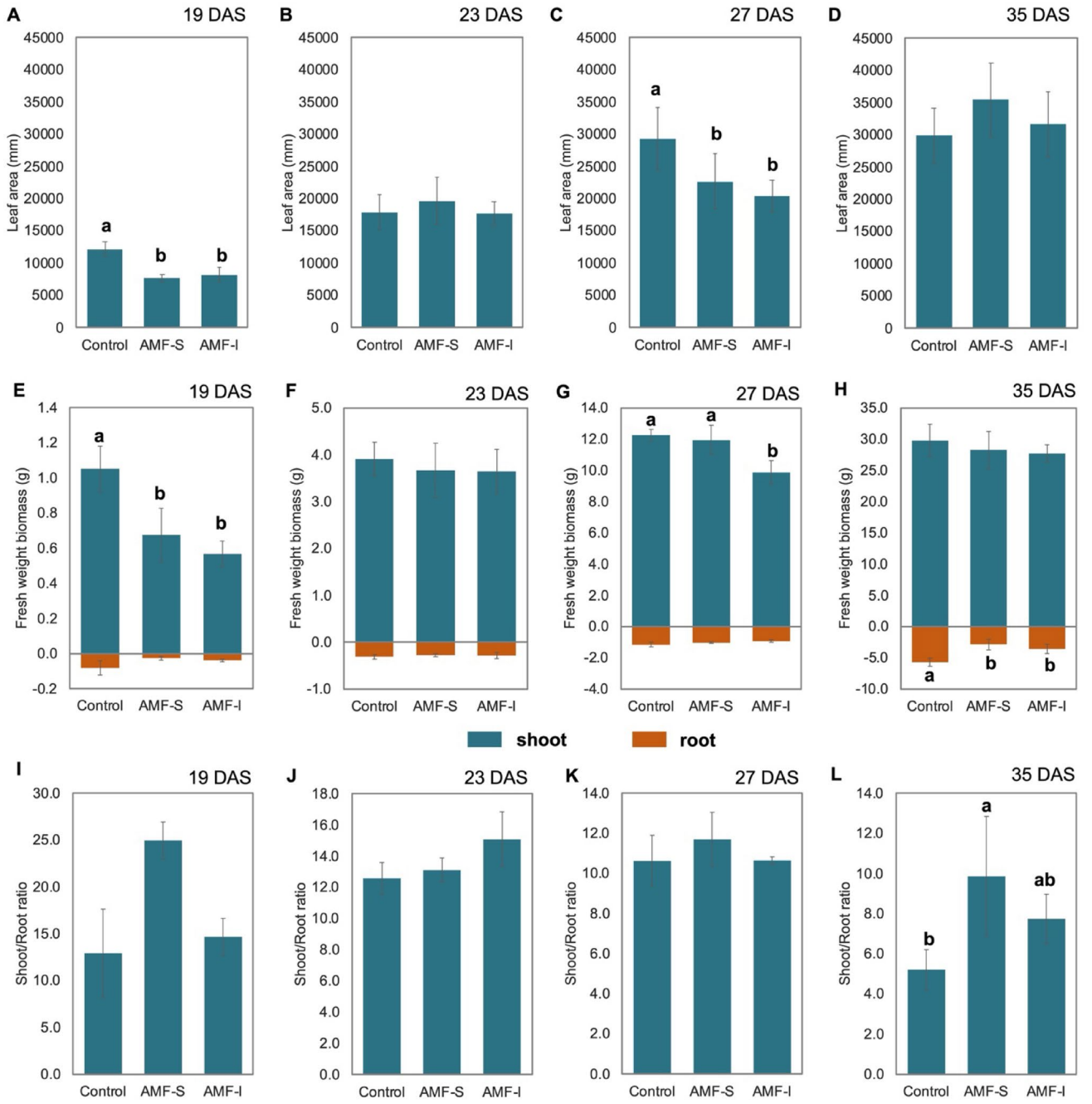

Fig. 1 Leaf area measurements [A-D], shoot and root fresh weight (FW) [E-H], and shoot/root ratio of tomato plants treated with Arbuscular Mycorrhizal Fungi by inoculation and seed-priming compared to control untreated at 19, 23, 27, and 35 days after sowing (DAS). All data are expressed as the mean ± standard deviation, $n = 3$. Different letters indicate analysis of variance (p-value < 0.05) + Tukey's post hoc test ($p = 0.05$)

In contrast, AMF-S plants maintained stable photosynthetic performance Fv/Fm_{max}, suggesting that AMF colonisation contributed to sustaining the efficiency of light energy conversion under these conditions. Regarding AMF-I plants, a lower photosynthetic performance was reported compared to AMF-S plants, with Fv/Fmmax values ranging from 0.79 to 0.80 (Fig. 2A). Interestingly, at 23 DAS, the AMF-I resulted in a lower capacity of the light dissipation process of excess energy under high light intensity conditions (Fig. 3B), suggesting a specific energy distribution at the onset of mycorrhization with roots.

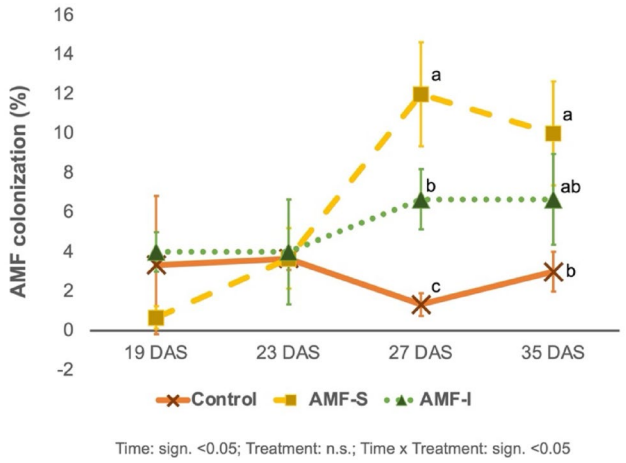

Fig. 2 Percentage of Arbuscular Mycorrhizal Fungi (AMF) colonization related to tomato plants treated with AMF by inoculation (AMF-I) and seed-priming (AMF-S) compared to the control at 19, 23, 27, and 35 days after sowing (DAS). All data are expressed as mean ± standard deviation, $n = 3$. Different letters within each DAS indicate analysis of variance (p-value < 0.05) + Tukey's post hoc test ($p = 0.05$). No letter indicates a lack of significant difference

Root Length and Morphology Are Affected by AMF

In agreement with the data obtained from the biomass, the root system was reported to have a very different development between the control and the AMF-treated plants. The total length of the roots, the surface area, the average diameter, and the volume of the roots were determined to investigate the morphological changes induced by the interaction of AMF during the early stage of growth. In general, greater root development was observed in control plants than in mycorrhized plants, with significant differences starting from 27 DAS (Table 1) and particularly at 35 DAS. In detail, at 27 DAS, root length and surface area were lower under AMF-I application compared to control and AMF-S treatments. However, at 35 DAS, both AMF-I and AMF-S-treated roots were less developed than the control, suggesting the beginning of a symbiotic process that, under non-stress conditions, results in energy redistribution caused by the symbiote. This hypothesis was also confirmed by the average diameter and volume of the roots, which were consistently lower in AMF-treated roots than in the control, especially at later time points (Table 1).

Untargeted Metabolomics in Roots Shows Differences Based on the Method of AMF Application

The root metabolome was investigated using an untargeted metabolomics approach through high-resolution mass spectrometry. The analysis allowed us to annotate 1934 putative metabolites, as listed in **Supplementary Table S3**, which includes comprehensive pathway classification, MS1 isotopic and MS/MS spectra, compound abundances, and

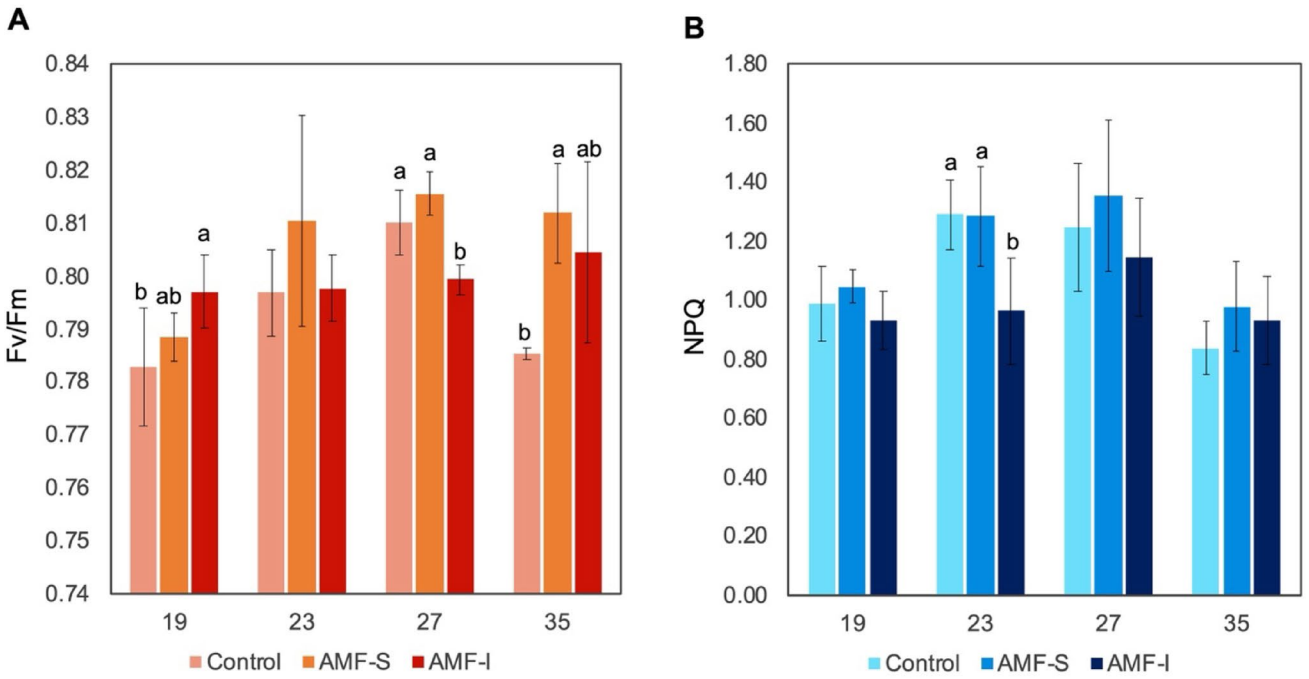

Fig. 3 Maximum quantum yield of the photosystem II (Fv/Fm) [A], and non-photochemical quenching (NPQ) parameters of tomato plant treated with Arbuscular Mycorrhizal Fungi by inoculation and seed-priming compared to control at 19, 23, 27, 35 days after sowing (DAS). All data are expressed as the mean ± standard deviation, $n = 6$. Different letters within each DAS indicate analysis of variance (p-value < 0.05) + Tukey's post hoc test ($p = 0.05$). No letter indicates no significant difference

Table 1 Root length, surface area, average diameter, and volume of tomato plants treated with arbuscular mycorrhizal fungi through inoculation and seed priming compared to untreated controls at 19, 23, 27, and 35 days after sowing

Time	Treatment	Total length (cm)	Surface area (cm^2)	Avg diameter (mm)	Root volume (cm^3)
19 DAS	Control	196.56 ± 75.51	14.69 ± 6.28	0.24 ± 0.01	0.09 ± 0.04
	AMF-S	118.68 ± 55.15	8.89 ± 4.00	0.24 ± 0.04	0.05 ± 0.03
	AMF-I	109.23 ± 20.64	9.50 ± 2.47	0.27 ± 0.02	0.07 ± 0.02
23 DAS	Control	630.48 ± 80.26	53.03 ± 6.16	0.27 ± 0.01 **a**	0.36 ± 0.04
	AMF-S	558.61 ± 95.47	43.36 ± 7.43	0.25 ± 0.00 **b**	0.27 ± 0.05
	AMF-I	553.26 ± 59.68	44.18 ± 5.98	0.25 ± 0.01 **ab**	0.28 ± 0.05
27 DAS	Control	1723.25 ± 165.72 **a**	166.77 ± 14.64 **a**	0.31 ± 0.00 **a**	1.28 ± 0.10 **a**
	AMF-S	1869.56 ± 188.69 **a**	168.44 ± 17.79 **a**	0.29 ± 0.00 **b**	1.21 ± 0.13 **b**
	AMF-I	1279.46 ± 101.11 **b**	122.36 ± 11.72 **b**	0.30 ± 0.00 **a**	0.93 ± 0.11 **ab**
35 DAS	Control	5777.14 ± 564.15 **a**	562.75 ± 55.38 **a**	1.04 ± 0.18 **a**	4.38 ± 0.44 **a**
	AMF-S	2992.06 ± 1006.54 **b**	292.77 ± 113.12 **b**	0.41 ± 0.18 **b**	2.28 ± 1.00 **b**
	AMF-I	4006.54 ± 483.58 **ab**	383.47 ± 38.58 **ab**	0.71 ± 0.16 **ab**	2.93 ± 0.23 **ab**

All data are expressed as the mean ± standard deviation, $n = 3$. Different letters indicate analysis of variance (p-value < 0.05) + Tukey's post hoc test ($p = 0.05$) within each time point. No letter indicates no significant difference. Abbreviation: Avg = Average, DAS = days after sowing

other information. Specifically, among the overall metabolites, 139 were also confirmed by MS/MS, and most of them belong to the lipid and fatty acid classes and secondary metabolites. The general similarities and dissimilarities among the samples were investigated using unsupervised HCA (Figure S1A), which clarified the strong influence of harvesting time on the root metabolome, and PCA (Figure S1B), which confirmed the HCA results and used to gain detailed insights into the effect of time on overall sample clustering, identifying a distinctive metabolic profile for 19 DAS plants (PC1). PC2 was primarily associated with discrimination among 23, 27 DAS, and 35 DAS plants. This result highlights how root metabolism changes over time, stabilizing when plant growth reaches a more stable state. Afterwards, based on the unsupervised models, a supervised ANOVA multi-blocking orthogonal projection to latent structures discriminant analysis (AMOPLS-DA) was performed to identify the specific data variance for each factor and their interaction (Fig. 4A).

The AMOPLS-DA analysis confirmed the PCA output concerning the harvest time factor, showing significant contributions of this factor to the explanation of the data variance with values of 50.9% relative sum of squares (RSS) (Fig. 4A). The discrimination between 19 DAS and late harvest time points was perfectly made by predictive component 1 (tp1 with 99.3%). In contrast, the 23 and 27 DAS harvest times were precisely discriminated against the last time point, 35 DAS, using tp2 (88.2%), as reported in the score plot (Fig. 4A). Regarding the AMF application factor, the model reported 3.7% of RSS values, making it the least explained factor by the model. The score plot distinguished the AMF-treated plant from the untreated one with the tp4 component (74.2%) and further differentiated between AMF-I and AMF-S using the tp8 component (63.8%). Interestingly, 9.1% of RSS was reported for the interaction between harvest time and AMF application factor, where tp3 and tp9 contributed to the different clusterization of the three treatments at the growth time point. In particular, the model highlighted a lower percentage of observed metabolomic differences that could not be explained by our factors, 36%, suggesting the reliability of our approach (Fig. 4A).

The importance of the harvest time factor and its interaction with the AMF application method was emphasised by conducting specific OPLS-DA models for each time point. This was carried out by comparing AMF-I vs. Control and AMF-S vs. Control to identify the VIP markers that were highly associated with discrimination between the pairwise comparisons. All OPLS-DA models demonstrated excellent fit and predictive capacity, along with cross-validated ANOVA results showing $p < 0.05$. The most discriminant metabolites, VIP > 1.3, were selected for each model and reported in the **supplementary Table S4**, together with log FC values.

The specific metabolic pathways were then built using these biomarkers, considering biosynthetic pathways and further delving into the secondary metabolite synthesis, separating AMF-S and AMF-I (Fig. 4B).

Regarding the modulation of root metabolism in AMF-S over the growing time, it has been observed that secondary metabolites were generally down-regulated, showing a stronger modulation at 19 DAS, highly contributed by isoprenoids and phenylpropanoids. Nonetheless, upon starting the mycorrhization from 23 DAS, a distinctive metabolic modulation was observed, particularly in a stronger down-modulation of carbohydrate biosynthesis, followed by an increased accumulation of lipids (fatty acids and steroids), and amino acids. Furthermore, considering secondary metabolites, an increased modulation of alkaloids, isoprenoids, lignans, and N-containing compounds was observed from 23 DAS, concurrent with the start of the mycorrhization process, suggesting the critical role of these compounds in plant-AMF communication (Fig. 4B). This time point

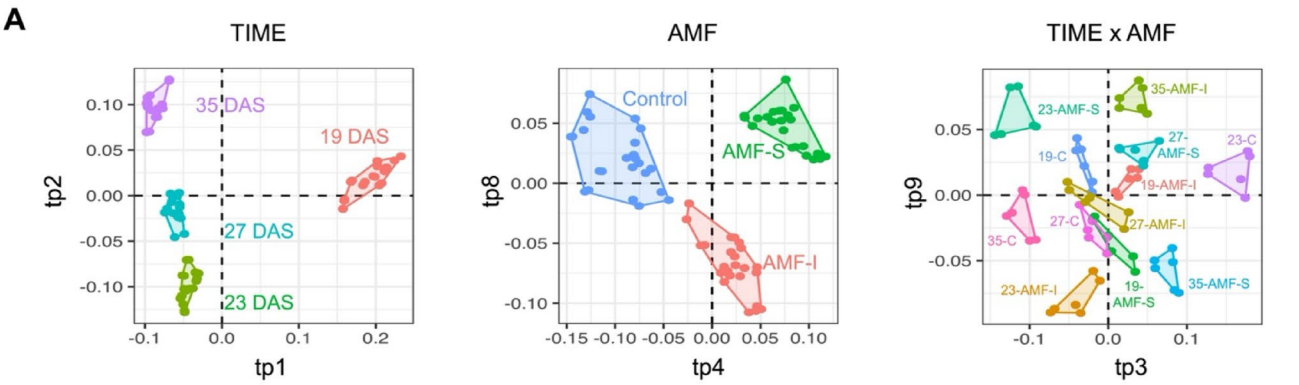

Effect Name	RSS	RSS p-value	R2Y p-value	Tp1	Tp2	Tp3	Tp4	Tp5	Tp6	Tp7	Tp8	Tp9	To1
Time	50.9%	0.033	0.033	99.3%	88.2%	2.4%	2.9%	3.0%	3.7%	43.3%	4.2%	4.4%	8.1%
AMF	3.7%	1.000	0.433	2.0%	3.9%	8.9%	74.2%	11.8%	17.6%	17.1%	63.8%	17.4%	30.9%
Time x AMF	9.1%	1.000	0.033	2.0%	3.6%	79.1%	10.5%	72.5%	59.3%	16.5%	14.1%	59.7%	27.8%
residuals	36.0%	-	-	2.0%	4.3%	9.6%	12.4%	12.5%	17.1%	16.3%	16.7%	19.0%	33.2%

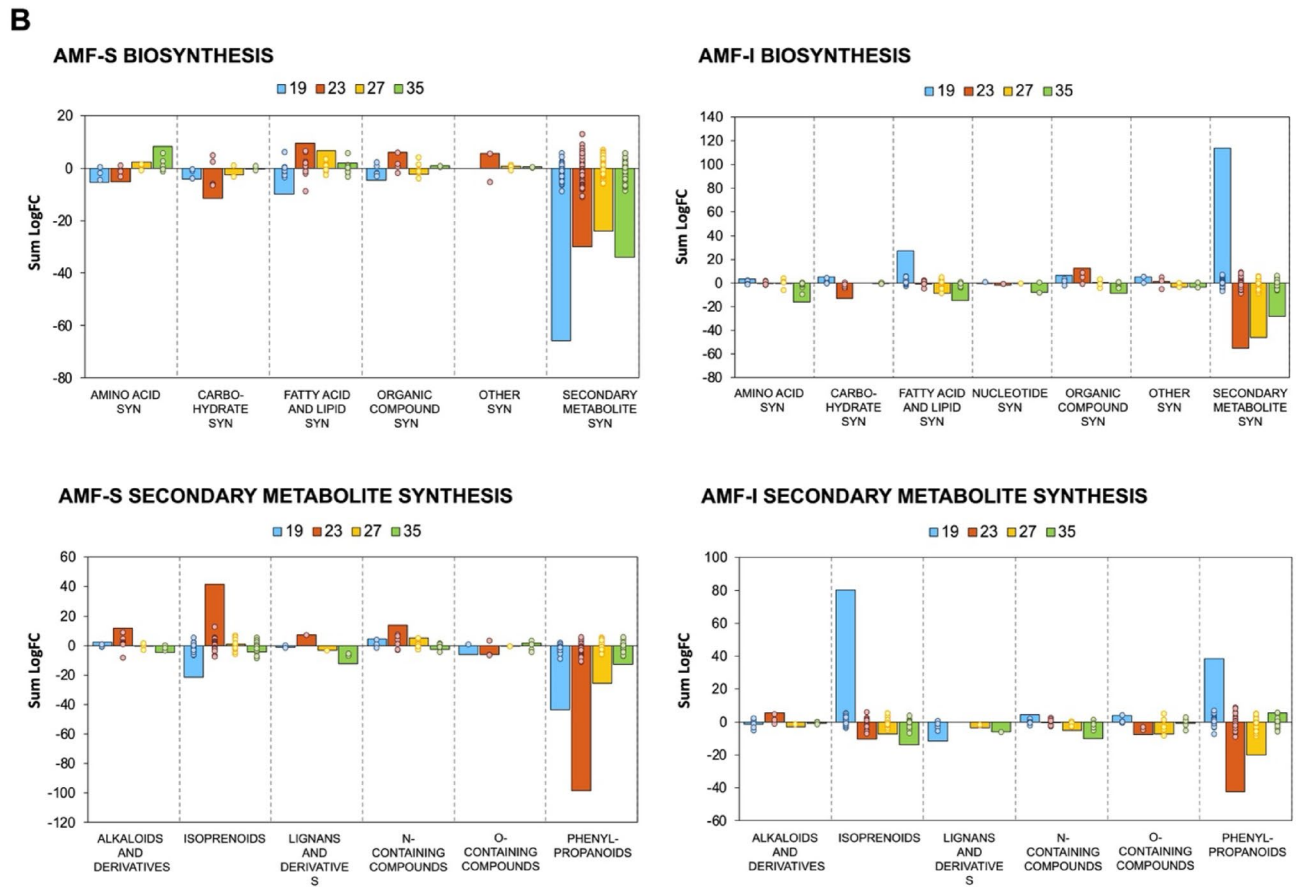

Fig. 4 **A**) Score plot and data table of ANOVA multi-blocking orthogonal projection to latent structures discriminant analysis of root metabolomic data subjected by different Arbuscular mycorrhizal Fungi (AMF) application – applied by seed priming (AMF-S) and by inoculation (AMF-I) compared to the control – different harvesting time (TIME) – 19, 23, 27, and 35 days after sowing (DAS) – and their interaction AMF x TIME. **B**) Pathway analysis of the most discriminant metabolites from the OPLS-DA model for biosynthesis and secondary metabolite synthesis pathways of tomatoes treated with AMF-I and AMF-S over the growing time. Abbreviations: RSS: Relative sum of squares, Tp1–9: predictive components, To1: orthogonal component. Syn: synthesis

was also characterized by a marked reduction in phenylpropanoid synthesis, indicating a redistribution of energy resources due to the establishment of symbiosis (Fig. 4B).

Concerning the modulation of root metabolism in AMF-I plants, it has been observed that secondary metabolites were again highly modulated compared to the other classes, indicating a peculiar metabolic response to the AMF colonization process. Interestingly, the metabolic response at 19 DAS produced an up-regulation of both primary and secondary metabolisms, resulting in the opposite trend compared to the AMF-S one. The difference in metabolic response could be related to a different way of root colonization according to the type of AMF application adopted. Specifically, amino acids (e.g., valine, isoleucine, and oligopeptides), carbohydrates, and fatty acids were up-accumulated compared to the control. However, by continuing with the AMF interaction with tomato root, an overall reduced metabolic activity was observed for the above classes, confirming the same outcome observed in AMF-S (Fig. 4B). Secondary metabolite production at 19 DAS was mainly characterized by isoprenoids, including mono-, di-, tri-, and sesquiterpenes. Then, phenylpropanoids were also reported to be up-regulated, including O-methylated and O-glycosylated flavonoids, tannins, and cinnamic acid. The following time points reported a metabolic trend similar to that observed for AMF-S.

Effect of Different AMF Applications on Tomato Plants' Exudation Profile

The root exudation profile during the mycorrhisation process was also investigated using UHPLC/IM-QTOF-MS to highlight the differences between the two modes of AMF application throughout the tomato growing period. The extensive exudate profile allowed us to detect 2,143 metabolites, as detailed in **supplementary table S5**, including pathway classification, MS1 isotopic and MS/MS spectra, compound abundances, and additional information on compound annotation.

The overall exudate profile was evaluated using unsupervised models (HCA and PCA; Figure S2) and supervised AMOPLS-DA to discriminate the harvest time, the AMF application method, and their interaction factors (Fig. 5A). Similar to the root metabolomics profile, the harvest time exhibited the highest RSS value (50.7%), indicating that the overall variance in the dataset was related to the plant stage. Specifically, harvest times were differentiated by predictive components 1 and 5 (99.3% and 88.1%, respectively). On the contrary, for the AMF application factor, the model accounted for 4.3% of the RSS values, making it the secondary discrimination factor, followed by the interaction between harvest time and the AMF application method. Regarding the VIP^2 biomarkers associated with each AMOPLS-DA model, a complete list of the 50 most influential metabolites is provided in the **supplementary table S6**.

Figure 5B shows the number and classes of VIP^2 biomarkers selected for each model. As reported, the impact of harvest time was characterized by the secretion of nitrogen-containing compounds (NCC; 11 metabolites) and phenylpropanoids (8 metabolites), followed by isoprenoids and alkaloids (6 metabolites for each). Among NCC, indoles, quinolines, and their derivatives were predominantly represented, while phenylpropanoids included small phenolics. Regarding the application of AMF, the root exudates were enriched with phenylpropanoids (22 metabolites), comprising coumarins, furanocoumarins, flavonoids, isoflavonoids, and phenolic acids, and isoprenoids (11 metabolites), mostly mono- di- tri- and tetraterpenoids. The time x AMF factor, aside from phenylpropanoids and isoprenoids, reported the accumulation of amino acids, carbohydrates, lipids, and phytohormones (salicylic acids).

To examine each time point in detail, single data comparisons vs. control were carried out to assess specific metabolite exudation at each time point. Specifically, the data were filtered using statistical analysis based on pairwise comparisons between AMF-treated samples and controls at each time point, and the log fold change modulation was calculated. The filtered metabolites were subsequently analyzed using ChemRICH to emphasize the enriched chemicals that changed significantly due to the association of AMF compared to the control. The resulting output plots and enrichment tables are reported in **Supplementary Materials** (**Figure S2 and Table S7**). Specifically, the ratio of increased to decreased metabolites from enriched classes of compounds was displayed in a heatmap (Fig. 6), separated by AMF-S (Fig. 6A) and AMF-I (Fig. 6B) application modes during the growth periods.

The AMF-S plants reported an increased class of enriched chemicals, 44 classes, compared to the inoculated one, 30 classes, suggesting an effective communication process when AMF was presented on the seed surface. Specifically, AMF-S increased pyran exudation during the early interaction stage (19 DAS), continuing the induction of other classes of metabolites until 23 DAS, including anthracyclines, benzylisoquinolines, furocoumarins, hydrolysable tannins, and pyrones. After 35 DAS, the consolidation mechanism produced an increased accumulation of diterpenes, flavanones, glucosides, hydroxybenzoates, and pyrones (Fig. 5A).

Regarding AMF-I, a spread-down accumulation of the main metabolite classes was observed until 27 DAS. The differential exudation pattern was observed at 35 DAS by inducing the secretion of chromones, cinnamates, coumarins, diterpenes, flavonoids, glucosides, iridoid glucosides, and lignans (Fig. 5**AB**).

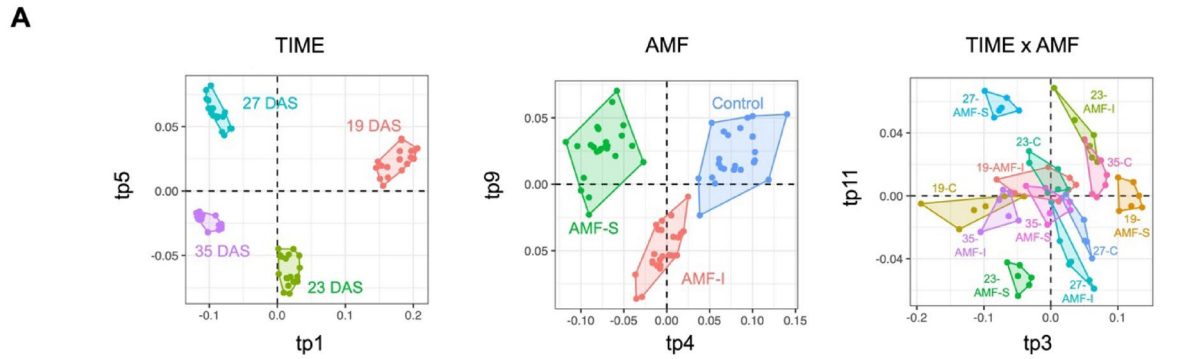

Effect Name	RSS	RSS p-value	R2Y p-value	Tp1	Tp2	Tp3	Tp4	Tp5	Tp6	Tp7	Tp8	Tp9	Tp10	Tp11	To1
Time	50.7%	0.01	0.12	99.3%	88.1%	1.6%	1.3%	91.6%	4.1%	3.9%	4.4%	4.2%	4.5%	3.2%	8.4%
AMF	4.3%	0.01	0.01	0.2%	3.8%	5.5%	88.7%	2.7%	14.2%	13.5%	15.5%	64.3%	15.5%	11.0%	29.1%
Time x AMF	9.6%	0.01	0.01	0.2%	3.6%	86.4%	4.4%	2.5%	64.8%	66.4%	61.6%	13.9%	61.4%	72.6%	27.7%
residuals	35.4%	-	-	0.3%	4.3%	6.6%	5.5%	3.2%	17.0%	16.2%	18.5%	17.6%	18.6%	13.2%	34.9%

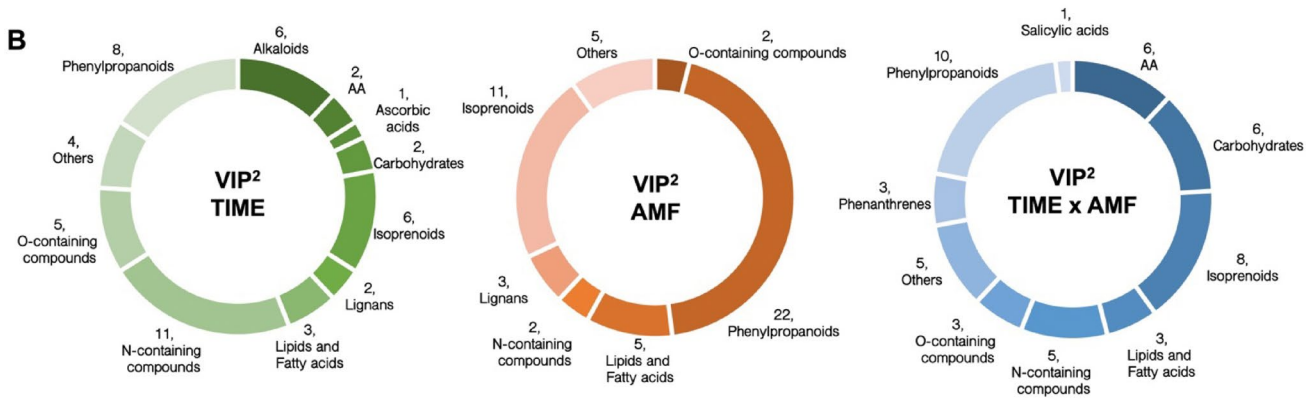

Fig. 5 **A**) Score plot and data table of ANOVA multi-blocking orthogonal projection to latent structures discriminant analysis (AMOPLS-DA) of root exudate profiles subjected to different Arbuscular mycorrhizal Fungi (AMF) applications – applied by seed priming (AMF-S) and by inoculation (AMF-I) compared to the control – different harvesting time (TIME) – 19, 23, 27, and 35 days after sowing (DAS) – and their interaction AMF x TIME. **B**) Pie chart of the variables of importance in projection (VIP^2) selected from each AMOPLS-DA model. Abbreviations: RSS: Relative sum of squares, Tp1–11: predictive components, To1: orthogonal component. AA: amino acids

Discussion

AMFs are widely recognised microbial biostimulants due to their ability to improve plant growth, productivity, and resilience to a variety of biotic and abiotic stresses, through the formation of symbiotic relationships with plants, extending the root system's capacity to access water and nutrients while receiving carbon sources from the plant in return (Gianinazzi et al. 2010).

While the long-term benefits of AMF have been extensively documented, their initial effects on plants, particularly in the absence of stress, have not been thoroughly explored (Gianinazzi et al. 2010; Birhane et al. 2012; Calvo et al. 2014). This study aims to bring to light an underexplored aspect of AMF interaction, its role in stress-free environments, by considering two different methods of AMF application, seed priming and inoculation at the transplanting stage, and four time points (19, 23, 27, and 35 DAS) to fill the gap in understanding the mechanism of symbiotic establishment at an early stage. The results reveal dynamic effects of AMF on tomato plant development. This temporally delayed response suggests that AMF colonization may function as a priming signal rather than an immediate modulator of plant physiology. Our time-resolved approach reveals that physiological and metabolic recovery in AMF-treated plants follows, rather than coincides with, the onset of colonization - indicating a functional decoupling not previously reported in tomato.

At 19 DAS, AMF-treated plants exhibited significantly reduced shoot biomass and leaf area compared to controls,

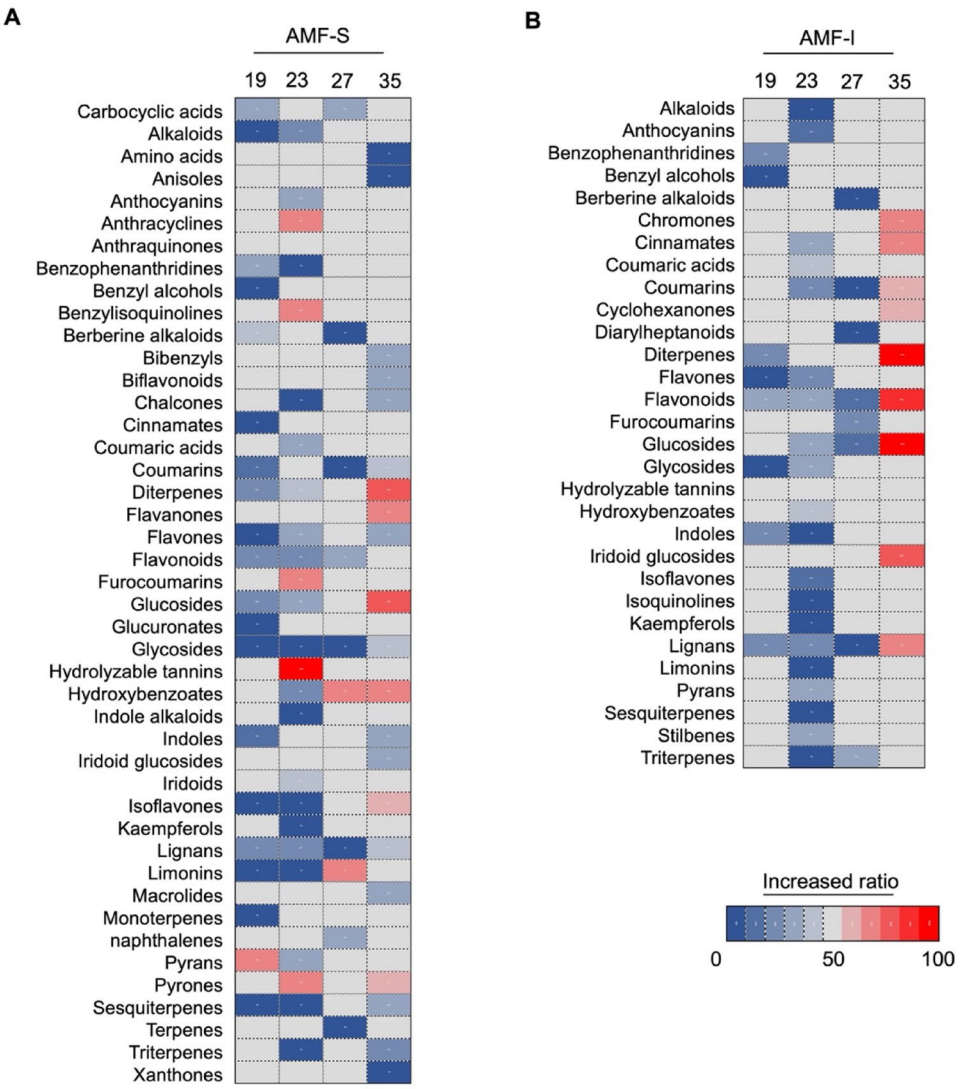

Fig. 6 Heat map of increased ratio values derived from results of chemical similarity enrichment analysis (ChemRICH) of tomato root exudates, which were differentially modulated after AMF treatment over time (19, 23, 27, and 35 days after sowing), distinguished by method of application: **A**) seed priming and **B**) inoculation at transplanting

with the inoculated being the most metabolically demanding in establishing symbiosis. Indeed, as reported by the AMF colonization data, a faster interaction between AMF and tomato root has been observed compared with seed priming, reporting 4% of root colonization against nearly 1%, respectively. Recent research has highlighted that during the early stages of symbiosis establishment, especially in the first month of plant life, AMF can negatively impact plant growth, due to the energy costs associated with the establishment of a symbiotic partnership (Arcidiacono et al. 2024). However, while studies in maize and barley have reported rapid microbial and physiological shifts within the first week post-inoculation (Begum et al. 2019; Jerbi et al. 2022), our findings suggest a slower and more energy-intensive transition in tomato, possibly due to species-specific traits or the inoculation method. Specifically, this interaction requires a metabolic investment from the plant, primarily in the form of carbon allocation from different organ parts to the root systems and then by modifying the tricarboxylic acid cycle (Kaur and Suseela 2020). This phenomenon initially inhibits the host's defense response; however, it prepares the host for enhanced defense against biotic and abiotic stresses by reprogramming the biosynthesis of primary and secondary metabolites (Menge 2023). Indeed, the higher AMF colonization of AMF-I was also associated with a significant increase in leaves' photosynthetic performance and the root system's metabolic activities. Accordingly, while a general down-regulation of root metabolism has been reported in AMF-S at 19 DAS, an overall up-regulation of both primary metabolisms, including amino acids (e.g., valine, isoleucine, and oligopeptides), carbohydrates, and fatty acids, and secondary metabolisms, mainly characterised by isoprenoids, including mono-, di-, tri- and sesquiterpenes and phenylpropanoids including *O*-methylated and *O*-glycosylated flavonoids, tannins, and cinnamic acid, was observed in AMF-I. The AMF-induced modulation of plant

metabolism was additionally confirmed by several studies, mainly reporting the up-regulation of the phenylpropanoid pathway in the synthesis of flavonoid class of compounds as chemical signals during the pre-symbiotic and symbiotic association stages (Chen et al. 2013; Kaur and Suseela 2020; Wang et al. 2024). The exudation profile of tomato plants at 19 DAS was characterized by a lower chemical enrichment, confirming the induction of plant metabolic activities on the onset of AMF-plant interaction for both AMF application methods. However, an increase in the release of organic acids has been observed for tomato plants treated with AMF at the 19 and 23 DAS compared to controls, particularly for citric acid, suggesting the elicitation of plant metabolism for AMF recognition and subsequent colonization (Zhang et al. 2025).

The recovery of the "downshift" in plant development and performance began at 23 DAS, where no significant decrease in plant biomass development was observed in the AMF-treated plants, suggesting an early interaction stages before the establishment of a balance plant-AMF symbiosis. Specifically, despite the decline in the non-photochemical quenching value reported for AMF-I-treated plants, no differences in photosynthetic performance among treatments were observed. This outcome validated the excess energy expense during the stages of symbiotic association with AMF-I (Moustakas et al., 2020), with consequent down-regulation of the main metabolic pathways, especially in secondary metabolism for the biosynthesis of phenylpropanoids, isoprenoids, and *O*-containing compounds at 23 DAS (Kaur and Suseela 2020). Conversely, seed-primed AMF showed an increase in the biosynthesis of fatty acids, organic compounds, and secondary metabolites (alkaloids, isoprenoids, lignans, and N-containing compounds). Unlike AMF-I, where inoculation occurs at the transplant stage and induces a strong metabolic modulation, the interaction in AMF-S is more gradual, allowing the symbiotic association to develop progressively. This controlled establishment minimises excessive metabolic shifts, ensuring a balanced resource allocation that, over time, leads to greater benefits for the plant without the intense metabolic cost observed in AMF-I. Interestingly, recovery of plant metabolism and performance in AMF-S was directly associated with the exudation of hydrolyzable tannins, furocoumarins, and benzylisoquinolines. At the same time, it was not observed in the case of AMF-I. An increase in exudation activity by tomato plants treated with AMF-S could be linked to a higher degree of mycorrhization at subsequent time points (27 and 35 DAS). In agreement with VIP^2 biomarkers selected for AMF treatment and time x AMF treatment factors, the root exudates were enriched with phenylpropanoids, comprising coumarins, furanocoumarins, flavonoids, isoflavonoids, and phenolic acids, and isoprenoids, mostly mono- di- tri- and tetraterpenoids, amino acids, carbohydrates, lipids, and phytohormones (salicylic acids).

During the early establishment of AMF association, plants often transiently activate defence-related pathways because the host initially cannot discriminate whether the colonising microbe is beneficial or pathogenic. This early response is typically attenuated once the symbiosis is recognised as beneficial and nutrient exchange begins (Enebe and Erasmus 2023). In this context, the accumulation of coumarins and furanocoumarins observed in our study likely reflects this initial recognition phase and their role in the regulation of fungal populations in the rhizosphere during the onset of colonisation (Prusty and Kumar 2019). These secondary metabolites realise were then coupled with sugar exudation during the AMF onset, playing a crucial role in the symbiotic relationship between plants and AMF and acting as a primary carbon source for fungi. Plants allocate significant amounts of photosynthetically produced sugars to their roots, which AMF use to promote their growth and function (Wang and Wu 2023), as well as amino acids and lipids (Canarini et al. 2019; Kameoka and Gutjahr 2022). Furthermore, we observed the exudation of phytohormones, particularly salicylic acid, found from literature as essential for regulating the symbiotic association (Gao et al. 2025). Salicylic acid collaborates with jasmonic acid throughout both the initial colonization and maintenance phases (García-Garrido and Ocampo 2002), ensuring successful interactions and maintenance of beneficial collaboration rather than an invasive colonization through the production of secondary metabolites such as flavonoids and terpenoids to control competing fungal growth (Adolfsson et al. 2017; Zambelli et al. 2025). Interestingly, Quiroga et al. (2018) showed a negative correlation between the rate of AM colonization and salicylic acid content in rise during the early stage of AMF colonization (Quiroga et al. 2018).

At 27 DAS, plant biomass nearly doubled compared to the previous time point, indicating the onset of the active growth phase and the successful establishment of mycorrhization for both AMF application methods, especially in seed-primed plants. Notably, AMF-S reached its peak colonization level, surpassing AMF-I in terms of fungal integration. During this stage, AMF-S-treated plants exhibited a marked increase in primary metabolites, such as amino acids and fatty acids. In contrast, AMF-I-treated plants showed a different trend, with compromised growth rate, photosynthesis efficiency, and metabolic activity. This reflects the initial "metabolic cost" of symbiosis in AMF-I, which alters a fast transition of symbiosis to a net benefit relationship.

At 35 DAS, shoot biomass was normalized across treatments, but AMF-treated plants showed reduced root fresh weight, suggesting resource redistribution favoring shoot growth and fungal symbiosis maintenance. This mechanism

could be explained by the fact that in the absence of a stress factor, plants face challenges in maintaining AMF symbiosis for future and eventual benefits, as they allocate approximately 4–20% of photosynthetically fixed carbon to AMF (Jung et al., 2012) in the form of sugars (Salmeron-santiago et al. 2021) and lipids (Keymer et al., 2017). In accordance, at 35 DAS, AMF-treated plants exhibited a higher number and quantity of exuded compounds compared to control, especially phenylpropanoids, diterpenes, and glucosides, which are essential for maintaining fungal symbiosis (Wang et al. 2024). Both application methods led to the accumulation of these metabolites, with AMF-I showing a higher amount than AMF-S, likely due to a slower association process caused by the initial "metabolic cost" and the need for more time to complete AMF association. In contrast, AMF-S-treated plants displayed a broader range of differentially expressed compounds, including higher concentrations of isoflavones, hydroxybenzoates, and pyrones, which are strictly linked to physiological adjustments occurring during the AMF establishment. These metabolites are commonly associated for the AMF spore germination, hyphae attraction to root and maintaining the stability of the mycorrhizosphere, such as flavonoids (Pei et al. 2020), phenolic acids (Li et al. 2023), and coumarins (Yang et al. 2024). These results highlight the temporary challenges of early AMF interaction and the eventual benefits, emphasizing the importance of the AMF application method for an optimal growth outcome. Moreover, they may improve the design of microbial consortia and application strategies for horticultural crops. In particular, early AMF application through seed priming appears to support a smoother integration, reducing initial metabolic stress and enabling a more stable functional symbiosis in tomato.

Conclusions

In conclusion, our study demonstrates that AMF colonization in tomato is a dynamic process, marked by an initial metabolic cost followed by functional recovery and benefits. The method and timing of application critically shape this trajectory. These findings enhance our understanding of early mycorrhization phases and offer insights for optimizing inoculation protocols to improve plant resilience and productivity.

The results demonstrated that the early interaction of AMF imposes a metabolic cost on tomato plants, particularly at 19 DAS, where the treated plants showed reduced shoot biomass and leaf area, and the inoculated plants faced greater metabolic demands. Root colonization progressed more rapidly in inoculated plants than in seed-primed ones. Metabolomic analyses confirmed that AMF modulates plant metabolism, redirecting carbon allocation and adjusting metabolic pathways to establish a functional symbiosis. By 23 DAS, adaptive responses were observed, with plants recovering from initial growth suppression. Seed-primed plants demonstrated a more gradual metabolic transition, allowing balanced resource allocation, while inoculated plants experienced pronounced metabolic shifts. At 27 DAS, AMF-treated plants entered an active growth phase, with seed-primed plants exhibiting peak colonization and metabolic benefits. By 35 DAS, shoot biomass was comparable between treatments, but AMF-associated root development remained altered, favouring the maintenance of symbiosis. These findings underscore the importance of the timing of AMF application and demonstrate their dynamic impact on plant physiology. While early interactions impose metabolic costs, proper management of AMF inoculation can optimize symbiosis establishment, ultimately supporting plant development and improving agricultural sustainability.

Supplementary Information The online version contains supplementary material available at https://doi.org/10.1007/s00344-026-12107-0.

Acknowledgements The authors thank the "Romeo ed Enrica Invernizzi" foundation (Milan, Italy) for supporting the metabolomics facility at Università Cattolica del Sacro Cuore and Athens, Agrotecnologia Naturales SL, for providing us with mycorrhizal products.

Author Contributions **Ilaria Ragnoli**: Writing – original draft, Software, Methodology, Formal analysis, Data curation. **Leilei Zhang**: Writing – original draft, Validation, Software, Methodology, Formal analysis, Supervision, Data curation, Conceptualization. **Florencia Asinari**: Writing – original draft, Validation, Software, Formal analysis, Data curation. **Tito Caffi**: Writing – review & editing, Supervision, Resources, Methodology, Data curation. **Luigi Lucini**: Writing – review & editing, Supervision, Resources, Data curation, Conceptualization.

Funding Open access funding provided by Università Cattolica del Sacro Cuore within the CRUI-CARE Agreement. I.R. and F.A. received a fellowship from the Doctoral School on the Agro-Food System (AgriSystem) of the Università Cattolica del Sacro Cuore (Piacenza, Italy). This research received no specific grant from funding agencies in the public, commercial, or not-for-profit sectors.

Data Availability Data will be made available on request. The supplementary data will be available on the Mendeley Data platform with this doi: https://doi.org/10.17632/msvk56cx4m.1.

Declarations

Competing Interests The authors declare that they have no known competing financial interests or personal relationships that could have appeared to influence the work reported in this paper.

References

Adolfsson L, Nziengui H, Abreu IN, Šimura J, Beebo A, Herdean A, Aboalizadeh J, Široká J, Moritz T, Novák O, Ljung K, Schoefs B, Spetea C (2017) Enhanced secondary- and hormone metabolism in leaves of arbuscular mycorrhizal *Medicago truncatula*. Plant Physiol 175:392–411

Arcidiacono M, Pellegrino E, Nuti M, Ercoli L (2024) Field inoculation by arbuscular mycorrhizal fungi with contrasting life-history strategies differently affects tomato nutrient uptake and residue decomposition dynamics. Plant Soil 500:105–127

Begum N, Ahanger MA, Su Y, Lei Y, Mustafa NSA, Ahmad P, Zhang L (2019) Improved Drought Tolerance by AMF Inoculation in Maize (Zea mays) Involves Physiological and Biochemical Implications. Plants 2019, Vol 8, Page 579 8: 579

Birhane E, Sterck FJ, Fetene M, Bongers F, Kuyper TW (2012) Arbuscular mycorrhizal fungi enhance photosynthesis, water use efficiency, and growth of frankincense seedlings under pulsed water availability conditions. Oecologia 169:895–904

Bona E, Cantamessa S, Massa N, Manassero P, Marsano F, Copetta A, ... Berta G (2017) Arbuscular mycorrhizal fungi and plant growth-promoting pseudomonads improve yield, quality and nutritional value of tomato: a field study. Mycorrhiza 27(1):1–11

Bravo A, Brands M, Wewer V, Dörmann P, Harrison MJ (2017) Arbuscular mycorrhiza-specific enzymes FatM and RAM2 fine-tune lipid biosynthesis to promote development of arbuscular mycorrhiza. New Phytol 214:1631–1645

Calvo P, Nelson L, Kloepper JW (2014) Agricultural uses of plant biostimulants. Plant Soil 383:3–41

Canarini A, Kaiser C, Merchant A, Richter A, Wanek W (2019) Root exudation of primary metabolites: mechanisms and their roles in plant responses to environmental stimuli. Front Plant Sci 10:422679

Cargill RIM, Shimizu TS, Kiers ET, Kokkoris V (2025) Cellular anatomy of arbuscular mycorrhizal fungi. Curr Biol 35:R545–R562

Chen S, Jin W, Liu A, Zhang S, Liu D, Wang F, Lin X, He C (2013) Arbuscular mycorrhizal fungi (AMF) increase growth and secondary metabolism in cucumber subjected to low temperature stress. Sci Hortic 160:222–229

Corradi N, Bonfante P (2012) The arbuscular mycorrhizal symbiosis: origin and evolution of a beneficial plant infection. PLoS Pathog. https://doi.org/10.1371/journal.ppat.1002600

Delaeter M, Magnin-Robert M, Randoux B, Lounès-Hadj Sahraoui A (2024) Arbuscular mycorrhizal fungi as biostimulant and biocontrol agents: a review. Microorganisms. https://doi.org/10.3390/microorganisms12071281

Enebe MC, Erasmus M (2023) Susceptibility and plant immune control—a case of mycorrhizal strategy for plant colonization, symbiosis, and plant immune suppression. Front Microbiol 14:1178258

Gao Y, Huang S, Zhang J, Zhu L, Zhan B, Yu X, Chen Y (2025) JA signaling inhibitor JAZ is involved in regulation of AM symbiosis with cassava, including symbiosis establishment and cassava growth. J Fungi 11(8):601

García-Garrido JM, Ocampo JA (2002) Regulation of the plant defence response in arbuscular mycorrhizal symbiosis. J Exp Bot 53:1377–1386

Giachero ML, Marquez N, Gallou A, Luna CM, Declerck S, Ducasse DA (2017) An in vitro method for studying the three-way interaction between soybean, rhizophagus irregularis and the soil-borne pathogen fusarium virguliforme. Front Plant Sci 8:1033

Gianinazzi S, Gollotte A, Binet MN, van Tuinen D, Redecker D, Wipf D (2010) Agroecology: the key role of arbuscular mycorrhizas in ecosystem services. Mycorrhiza 20:519–530

Jerbi M, Labidi S, Laruelle F, Tisserant B, Dalpé Y, Lounès-Hadj Sahraoui A, Ben Jeddi F (2022) Contribution of Native and Exotic Arbuscular Mycorrhizal Fungi in Improving the Physiological and Biochemical Response of Hulless Barley (Hordeum vulgare ssp. nudum L.) to Drought. Journal of Soil Science and Plant Nutrition 2022 22:2 22: 2187–2204

Johnson R, Joel JM, Puthur JT (2024) Biostimulants: the futuristic sustainable approach for alleviating crop productivity and abiotic stress tolerance. J Plant Growth Regul 43:659–674

Jung SC, Martinez-Medina A, Lopez-Raez JA, Pozo MJ (2012) Mycorrhiza-induced resistance and priming of plant defenses. J Chem Ecol 38(6):651–664

Kameoka H, Gutjahr C (2022) Functions of lipids in development and reproduction of arbuscular mycorrhizal fungi. Plant Cell Physiol 63:1356–1365

Kaschuk G, Kuyper TW, Leffelaar PA, Hungria M, Giller KE (2009) Are the rates of photosynthesis stimulated by the carbon sink strength of rhizobial and arbuscular mycorrhizal symbioses? Soil Biol Biochem 41:1233–1244

Kaur S, Suseela V (2020) Unraveling arbuscular mycorrhiza-induced changes in plant primary and secondary metabolome. Metabolites 10:1–30

Kaya C, Higgs D, Kirnak H, Tas I (2003) Mycorrhizal colonisation improves fruit yield and water use efficiency in watermelon (Citrullus lanatus Thunb.) grown under well-watered and water-stressed conditions. Plant Soil 253(2):287–292

Keymer A, Pimprikar P, Wewer V, Huber C, Brands M, Bucerius SL, ... Gutjahr C (2017) Lipid transfer from plants to arbuscular mycorrhiza fungi. elife 6:e29107

Kiers ET, Van Der Heijden MGA (2006) Mutualistic stability in the arbuscular mycorrhizal symbiosis: exploring hypotheses of evolutionary cooperation. Ecology 87:1627–1636

Lee S, Hwang S, Seo M, Shin KB, Kim KH, Park GW, Kim JY, Yoo JS, No KT (2020) BMDMS-NP: a comprehensive ESI-MS/MS spectral library of natural compounds. Phytochemistry 177:112427

Li C, Deng Y, Wang J, Ruan W, Wang S, Kong W (2023) Effects of p-Hydroxyphenylacetic Acid and p-Hydroxybenzoic Acid on Soil Bacterial and Fungal Communities. Sustainability 2023, Vol 15, 15

Malhi GS, Kaur M, Kaushik P (2021) Impact of climate change on agriculture and its mitigation strategies: a review. Sustain (Switzerland) 13:1–21

Mcgonigle TP, Miller MH, Evans DG, Fairchild GL, Swan JA (1990) A new method which gives an objective measure of colonization of roots by vesicular—arbuscular mycorrhizal fungi. New Phytol 115:495–501

Menge E (2023) Investigating the ecological role of arbuscular mycorrhizal fungi (AMF) in natural ecosystems. Int J Sci Res Arch 10:524–534

Moustakas M, Bayçu G, Sperdouli I, Eroğlu H, Eleftheriou EP (2020) Arbuscular mycorrhizal symbiosis enhances photosynthesis in the medicinal herb Salvia fruticosa by improving photosystem II photochemistry. Plants 9(8):962

Paul K, Sorrentino M, Lucini L, Rouphael Y, Cardarelli M, Bonini P, Reynaud H, Canaguier R, Trtílek M, Panzarová K, Colla G (2019) Understanding the biostimulant action of vegetal-derived

protein hydrolysates by high-throughput plant phenotyping and metabolomics: A case study on tomato. Front Plant Sci 10:47

Pei Y, Siemann E, Tian B, Ding J (2020) Root flavonoids are related to enhanced AMF colonization of an invasive tree. AoB Plants 12:plaa002

Prusty JS, Kumar A (2019) Coumarins: antifungal effectiveness and future therapeutic scope. Molecular Diversity 2019 24:4 24: 1367–1383

Quiroga G, Erice G, Aroca R, Zamarreño ÁM, García-Mina JM, Ruiz-Lozano JM (2018) Arbuscular mycorrhizal symbiosis and Salicylic acid regulate Aquaporins and root hydraulic properties in maize plants subjected to drought. Agric Water Manage 202:271–284

Salmeron-santiago IA, Martínez-trujillo M, Valdez-alarcón JJ, Pedraza-santos ME, Santoyo G, Pozo MJ, Chávez-bárcenas AT (2021) An updated review on the modulation of carbon partitioning and allocation in arbuscular mycorrhizal plants. Microorganisms 10:75

Sudiro C, Guglielmi F, Hochart M, Senizza B, Zhang L, Lucini L, Altissimo A (2022) A phenomics and metabolomics investigation on the modulation of drought stress by a biostimulant plant extract in tomato (*Solanum lycopersicum*). Agronomy. https://doi.org/10.3390/agronomy12040764

Team RC (2021) R: A Language and environment for statistical computing. Available at https://www.r-project.org/

Team Rs (2020) RStudio: Integrated Development for R. Available At http://www.rstudio.com/

Wang Y-J, Wu Q-S (2023) Influence of sugar metabolism on the dialogue between arbuscular mycorrhizal fungi and plants. Horticulture Advances 2023 1:1 1: 1–12

Wang L, Xia Y, Hou Y (2024) Candy or poison: plant metabolites as swing factors against microbes. Mol Plant 17:1341–1343

Wu QS, Li GH, Zou YN (2011) Roles of arbuscular mycorrhizal fungi on growth and nutrient acquisition of peach (Prunus persica L. Batsch) seedlings. J Anim Plant Sci 21(4):746–750

Yang L, Qian X, Zhao Z, Wang Y, Ding G, Xing X (2024) Mechanisms of rhizosphere plant-microbe interactions: molecular insights into microbial colonization. Front Plant Sci 15:1491495

Zambelli A, Nocito FF, Araniti F (2025) Unveiling the Multifaceted Roles of Root Exudates: Chemical Interactions, Allelopathy, and Agricultural Applications. Agronomy 2025, Vol 15, 15

Zhang D, Liu X, Zhang Y, Ye J, Yi Q (2025) Effects of Arbuscular Mycorrhizal Fungi on the Physiological Responses and Root Organic Acid Secretion of Tomato (Solanum lycopersicum) Under Cadmium Stress. Horticulturae 2025, Vol 11, 11